Available online at www.sciencedirect.com
ScienceDirect
European Polymer Journal 43 (2007) 4136–4142
EUROPEAN POLYMER JOURNAL
www.elsevier.com/locate/europolj

Macromolecular Nanotechnology

Probing buried carbon nanotubes within polymer–nanotube composite matrices by atomic force microscopy

In Yee Phang [a,b], Tianxi Liu [c,*], Wei-De Zhang [d], Holger Schönherr [a], G. Julius Vancso [a,b,*]

[a] *MESA+ Institute for Nanotechnology, Department of Materials Science and Technology of Polymers, P.O. Box 217, 7500 AE Enschede, The Netherlands*
[b] *Dutch Polymer Institute, P.O. Box 902, 5600 AX Eindhoven, The Netherlands*
[c] *Key Laboratory of Molecular Engineering of Polymers of Chinese Ministry of Education, Department of Macromolecular Science, Fudan University, 220 Handan Road, Shanghai 200433, PR China*
[d] *Nano Science Research Center, College of Chemistry, South China University of Technology, Guangzhou 510640, PR China*

Received 20 April 2007; received in revised form 29 June 2007; accepted 4 July 2007
Available online 3 August 2007

Abstract

Multi-walled carbon nanotubes (MW-CNT) inside a polyamide-6 (PA6)–MW-CNT composite were visualized by atomic force microscopy (i) in a field-assisted intermittent contact and (ii) in the tunneling (TUNA) mode. Individual buried MW-CNTs were clearly discerned within the PA6 matrix. An average diameter of 33 ± 5 nm of the MW-CNTs was determined based on field-assisted intermittent contact mode AFM images, which is consistent with the expected size of PA6-coated MW-CNTs. Single well dispersed MW-CNTs that are located in the sub-surface region of the composite were also observed in the TUNA mode. These new AFM approaches circumvent the tedious sample preparation based on ultramicrotoming required for high resolution electron microscopy studies to obtain "in-depth" morphological information and hence are expected to facilitate the analysis of CNT-based and other nanocomposites in the future.

Keywords: Carbon nanotube composites; Atomic force microscopy; Conducting mode; TUNA mode; Nylon-6

1. Introduction

The discovery of fullerenes in 1985 [1] and carbon nanotubes (CNTs) in 1991 [2,3] opened up a new era in material science. Owing to their unique physical properties, such as high strength and stiffness, together with excellent thermal and electric conductivities, as well as low mass, CNTs have become a key candidate, among others, for future electronic materials and advanced nanocomposites. They are

* Corresponding authors. Address: MESA+ Institute for Nanotechnology, Department of Materials Science and Technology of Polymers, P.O. Box 217, 7500 AE Enschede, The Netherlands. Tel.: +31 53 4892967; fax: +31 53 4893823 (G.J. Vancso), tel.: +86 21 55664197; fax: +86 21 55664192 (T. Liu).
E-mail addresses: txliu@fudan.edu.cn (T. Liu), g.j.vancso@tnw.utwente.nl (G.J. Vancso).

0014-3057/$ - see front matter © 2007 Elsevier Ltd. All rights reserved.
doi:10.1016/j.eurpolymj.2007.07.035

considered to be ideal materials in various applications [4] such as nanofillers for the fabrication of composite materials [5], conductors in micro- and nano-electronics [6], as well as platforms for truly molecular electronics [7] and potential nano-transporters in nano-fluidic applications [8].

The synergistic combination of various polymers (e.g. poly(styrene), poly(methyl methacrylate), poly(vinyl alcohol), or polyamide-6) and CNTs can be exploited in high-performance, multifunctional composites [9–11]. However, many challenges still remain to be overcome, such as tailoring of the polymer–CNT interfaces and achieving maximum dispersion of high aspect ratio CNTs in highly loaded composites [12–14].

Transmission electron microscopy (TEM) is the most common high resolution microscopic technique for morphological studies of buried nanofillers, such as CNTs, within polymer matrices. Recently, the tomography of nanostructures was obtained in TEM experiments, in which additional spectra of energy-loss images were evaluated [15]. Additionally, other techniques, such as scanning near-field optical microscopy (SNOM), ultrasound holography and thermal emission microscopy have been used to obtain sub-surface information in a non-destructive manner. SNOM demonstrated the ability for probing the sub-surface regions of composites down to a depth of >80 nm combined with the acquisition of chemically specific information by collecting Raman spectra. However, most of these techniques require tedious sample preparation and special instrumental modification [16–19].

Alternatively, atomic force microscopy (AFM) has shown promise to study a broad range of materials with high spatial resolution down to the nanometer scale. In particular in heterogeneous systems, such as semicrystalline polymers, block copolymers or filled elastomers [20–25], materials contrast can be obtained in various imaging modes. Images of single wall CNTs on solid substrates can be easily obtained by intermittent contact (tapping) mode [26]. Even though intermittent contact mode [27] provides materials contrast in the phase imaging mode, and also some limited depth sensitivity [28,29], it is clear that new modes must be developed and applied to be able to study the dispersion of nanofillers in the *sub-surface regions* of composite materials [30].

In this paper we report on the application of two new AFM modes to reveal the morphology of MW-CNTs embedded in PA6–MW-CNT composite samples. In the first approach, using an electrical bias applied between the AFM cantilever/tip assembly and the sample, the distribution and size of sheathed MW-CNTs inside the polymer matrix were analyzed in the intermittent contact phase mode. Secondly, the tunneling AFM (TUNA) mode was applied to detect dispersed (conducting) MW-CNTs *inside* the polymer matrix by measuring a minute current passing between the conductive AFM tip and the sample [31–35]. These AFM techniques are shown to provide crucial morphological information both on the sub-surface structure of the composites and on buried MW-CNTs within the PA matrix (with an estimated probe depth up to ~several micrometers). The non-destructive AFM techniques applied here only require minimum sample preparation (compared with the tedious sectioning procedures for e.g. electron microscopy (EM)), yet are shown to provide results comparable to the other established techniques.

2. Experimental part

PA6 composites with 2 wt% MW-CNTs were prepared as reported previously [36,37]. A small amount of composite sample was cut from the as-prepared sample and melted at 250 °C in between a clean metal sample stub and a pre-cleaned glass cover slide. This sample preparation procedure results in direct contact between the PA6–MW-CNT composite sample and the metal stubs without the need to use a conducting glue. AFM measurements were carried out with a Dimension D3100 using a NanoScope IVa controller equipped with a hybrid 153 scanner and the TUNA application module (Veeco/Digital Instruments (DI), Santa Barbara, CA) in ambient conditions. Both silicon cantilevers (Nanosensors, Wetzlar, Germany) and a cobalt-coated silicon cantilever (MESP, Nanoprobes, DI) were used for intermittent contact (tapping) mode operation and TUNA measurement, respectively. In addition, a soft silicon cantilever ($k_c \sim 0.3$ N/m, μMasch, ultrasharp Si cantilever (model, CSC37/AIBS/3)) was used for the acquisition of force–displacement data. Scan rates were varied from 0.3 Hz to 1 Hz. In field-assisted AFM imaging, the electric bias was varied between the probe and substrate for each experiment. TUNA measurements were carried out in contact mode with disabled *x*-, *y*-feedback.

3. Results and discussion

AFM was first applied to probe the morphology and dispersion of MW-CNTs embedded in the PA6–MW-CNT composite. Fig. 1 shows simultaneously acquired height and phase images of the composite sample captured with different electrical biases applied between tip and sample.

The morphology of the composite with elongated thin features distributed evenly across the sample was clearly observed (refer to Fig. 1). These features, with a typical width of 12.5 ± 1.4 nm, are attributed to PA6 lamellae. These lamellae apparently could not organize into large spherulitic structures due to the high nucleation density caused by the known excellent nucleation ability of MW-CNTs [38]. In addition, unusual elevated dot-like structures (Fig. 1A) were observed scattered over the entire sample. The dot diameters ranged from 25 nm to 66 nm with an average diameter of 33 ± 5 nm.

In previous reports [36], similar dot-like features were observed by scanning electron microscopy and interpreted as protruding MW-CNTs. Hence it is reasonable to identify the observed features as individual MW-CNTs. The phase image in Fig. 1B shows that these dots have similar phase contrast as the thin PA6 lamellae, thus it is impossible to distinguish MW-CNTs from the matrix. When a different bias was applied between tip and sample, the height images remained almost undisturbed (Fig. 1C, E and G); however, many bright dots

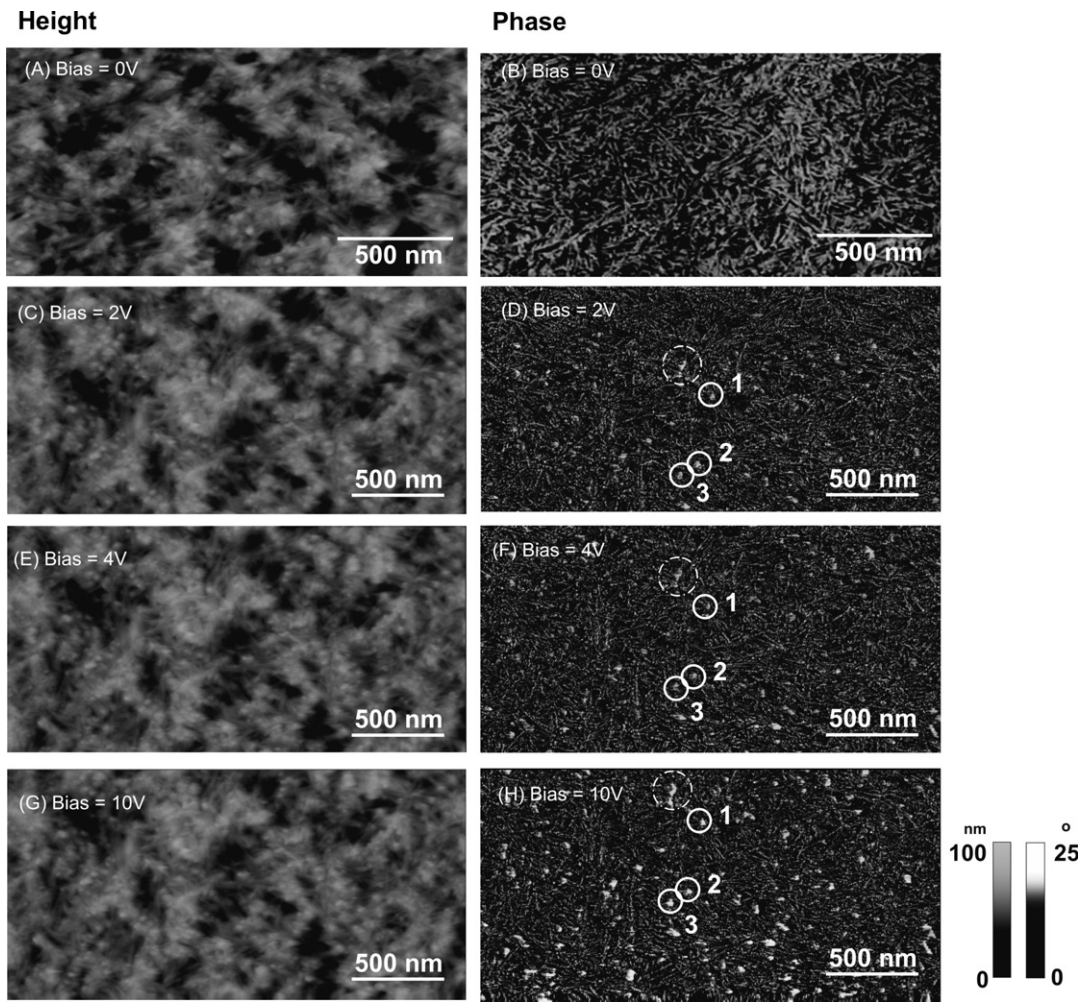

Fig. 1. AFM height (left) and phase (right) images acquired on a PA6 composite containing 2 wt% MW-CNT. The data were taken with a bias of (A, B) 0.0 V, (C, D) 2.0 V, (E, F) 4.0 V and (G, H) 10.0 V.

emerged across the sample in the phase images, as shown in Fig. 1D, F and H. The presence of artifact is unlikely because (i) consistent height images were observed throughout the experiments (Fig. 1C, E and G), and because (ii) the location of the bright spots (i.e., 1, 2, and 3 as labeled in Fig. 1D, F and H, respectively) remained unchanged even after increasing the bias from 2 V to 10 V.

The apparent contrast enhancement in the intermittent contact mode phase images can be attributed to different cantilever/tip–sample interactions. As shown in Fig. 2a and b the frequency and phase response of cantilever–sample interaction without (Fig. 2a) and with (Fig. 2b) the presence of bias is clearly different. Most notably, the phase response is sharper when a bias is present. This enhanced phase response coincides with increased attractive interactions detected in force–displacement curves (Fig. 2c), and agrees with a report by Tivanski and coworkers, who showed an increase of adhesion force in the presence of bias across the surface of gold grafted polythiophene [39,40]. Another reasonable conjecture is that the local bias leads to a softened surface, thereby enhancing the tip–sample interactions and concomitantly the phase contrast. This interpretation would be in line with the temperature-enhanced phase contrast observed in block copolymer samples [41].

Compared to conventional low vacuum SEM analyses of similar samples, our AFM micrographs showed higher coverages (five times higher than in SEM). Taking the sampling depth of intermittent contact mode AFM into account, this result shows that indeed the sub-surface regions of the composite have been probed.

The size of individual MW-CNTs observed by AFM (average value of 33 ± 5 nm) is significantly larger than that determined by TEM on thin sections of the composite (about 12 nm) (as reported previously in Ref. [37]) and TM-AFM on neat MW-CNTs dispersed on a solid substrate (18.4 ± 5.3 nm, see supporting information, Figure S1). This increase in diameter is confidently attributed to the presence of a thin layer of polymer surrounding the MW-CNT, as tip convolution effects affect the results to a much lower extent (compare numbers above). The presence of a thin matrix layer sheathing the MW-CNTs in polymer composites has been reported by Gass et al. [15]. This thin polymer layer is a major obstacle for conventional microscopy to identify individual MW-CNTs distributed inside such composites, unless the CNTs

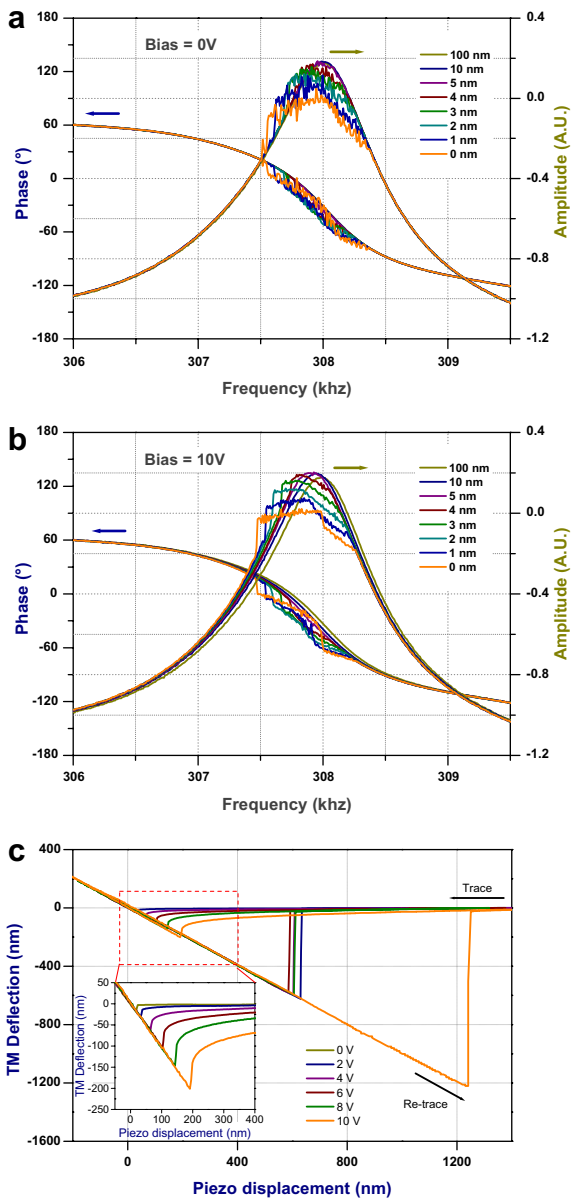

Fig. 2. Frequency and phase response of a Si cantilever on PA6 composite containing 2 wt% MW-CNT under different bias (a) 0 V and (b) 10 V. (c) Force–distance curves taken on PA6 composite containing 2 wt% MW-CNT using a soft silicon cantilever ($k_c \sim 0.3$ N/m, μMasch) illustrate the increasing attraction as bias increased across the tip and sample.

are visualized by TEM energy-loss spectroscopy or indirectly by SEM [15,36]. This thin polymer layer may also explain why the MW-CNTs were not observed in Fig. 1B, as the phase contrast between CNT and matrix is insignificant in the absence of an electronic bias under normal tapping mode

operation conditions. The presence of additional adhesion forces (as a result of the bias applied) enhances the tip–sample interactions in the tapping cycle and thereby local differences in energy dissipation can be revealed.

The MW-CNTs were also visualized in the TUNA mode, which is based on the measurements of the current between a conductive AFM tip and the sample (Fig. 3) [31]. Apart from the obvious applications in the area of semiconductors, metal-oxide films, and conducting polymers, the TUNA mode is most useful, as shown below, to analyze composites reinforced with conducting fillers [31–35]. Besides the previous mentioned technique to probe the sheathed MW-CNT, conducting AFM reported here also demonstrates the ability to visualize the dispersion of the buried MW-CNT in the polymer matrix.

The *height* image (Fig. 3A) shows the morphology of the PA6–MW-CNT composite with many dot-like structures. The non-centrosymmetric shapes are likely due to tip convolution effects stemming from the cobalt-coated AFM tip. Fig. 3B displays the corresponding TUNA *current* image of the composite sample, in which the dispersion of conducting MW-CNTs buried inside the polymer matrix is discernible. Buried MW-CNTs can successfully be visualized using an appropriate bias (in this case +5 V). The different contrast for different MW-CNTs within the matrix is associated with MW-CNTs located in different depths from the sample surface. An individual MW-CNT

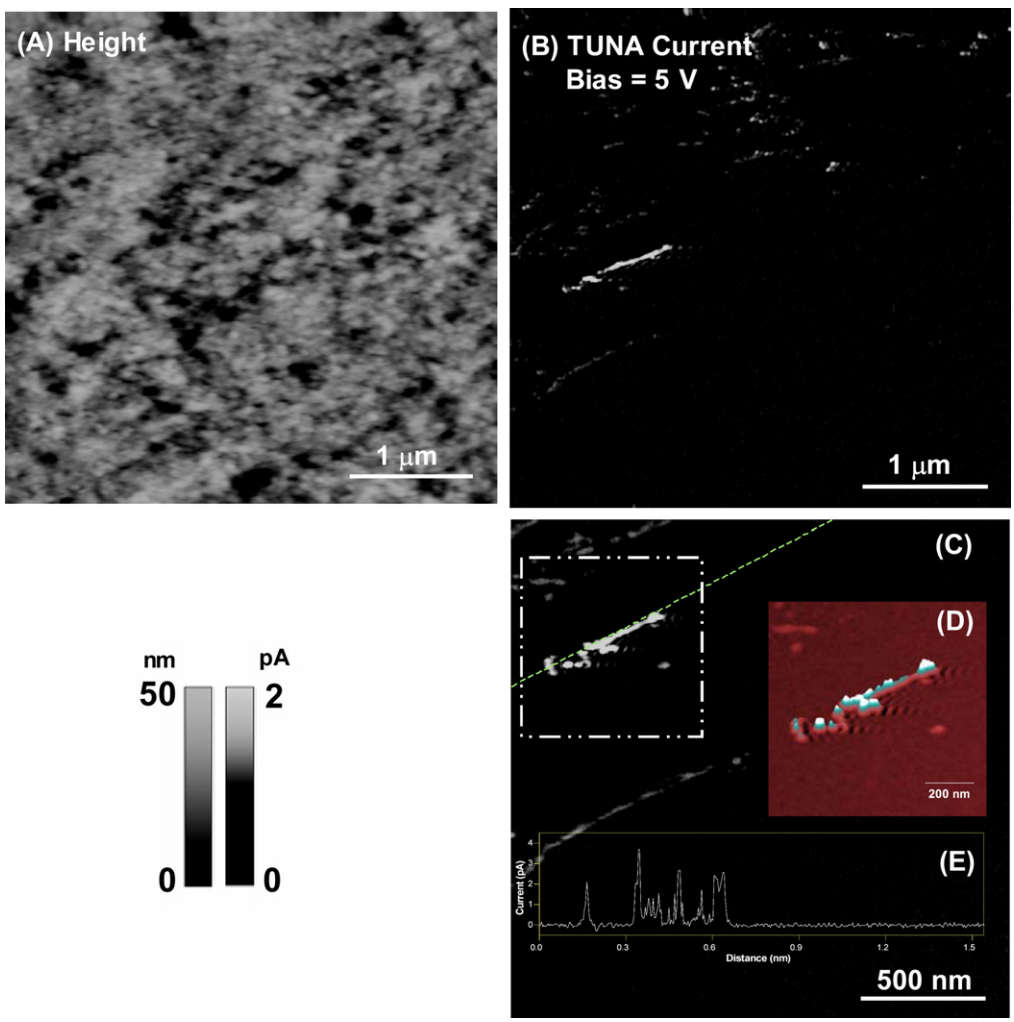

Fig. 3. Conducting AFM (TUNA mode) images of PA6–MW-CNT composite: (A) height image, (B) conducting current image, (C) zoomed region of (B), (D) perspective view of enlarged image as indicated in (C), and (E) the current profile along the dashed line in (C).

is highlighted in Fig. 3C. Several bright spots in the top left of Fig. 3C comprise very likely a cluster of MW-CNT dispersed in the PA6 matrix. The mean diameter determined from the analysis of cross-sectional plots of individual MW-CNTs was 37 ± 12 nm.

As for most force microscopy techniques, the resolution of TUNA is constrained by the size of the tip, which is significantly increased due to the granular metal coating. In addition to feature broadening, the presence of multiple cobalt particles attached to the tip apex led to double tip imaging, as was occasionally observed in the TUNA current images.

In thicker samples (for film thickness > 3 μm) no individual MW-CNTs were observed. Since the detected current depends sensitively on the plane where the MW-CNT is located, the current was in this case likely below the conducting threshold. If the MW-CNT is located at an optimum distance from the sample and the tip, respectively, i.e. in between two equal volumes of insulator that allows the conduction of current, a measurable conductivity change across the sample can be detected in TUNA (sensitivity down to 50 femto-ampere (50×10^{-15} A)). For other arrangements of the conducting CNT, the increased conducting barrier due to a non-equal distribution of the insulation layer will retard the current conduction [42–44]. This behavior can be explained by the electric conduction percolation theory, which states that the filler concentration and sample thickness play a significant role in conductivity measurement [43,44]. Low concentrations of well dispersed MW-CNTs with low degrees of network formation in the polymer matrix were shown to result in fewer available conducting pathway than in heavily loaded carbon-black composites. However, in our work, TUNA shows its extreme high sensitivity that allows local current sensing down to 1pA. TUNA is certainly an essential proximity probe microscopy mode for ultra-sensitivity local and nanoscale electric property measurements for conducting molecules and composites. If the sample can be prepared with a thickness down to scale of 100 nm by sectioning or electro-melt spinning [45], the tomography of individual MW-CNT in the composite sample could be obtained by varying the bias [15]. However, the preliminary results presented here show that TUNA is sensitive enough to locate buried MW-CNTs inside the composites. From Fig. 3D and E it can be concluded that this particular MW-CNT laid in different depths within the sample since the current profile varied significantly along the individual MW-CNT. An additional advantage of the TUNA mode over the conventional EM is its ability to measure the conductivity of the sample locally.

4. Conclusion

It can be summarized that the morphology of a PA6–MW-CNT composite was successfully unraveled by AFM in the intermittent contact (tapping) mode in the presence of an electric tip–sample bias, as well as in the TUNA mode. The dispersion of MW-CNTs in the composite sample was imaged with nanometer scale resolution and the diameter of individual CNTs was quantitatively determined. Future experiments will focus on the analysis of the three-dimensional distribution of MW-CNTs inside composites (tomography) of different thickness and the correlation with conductivity measurements.

Acknowledgements

The authors acknowledge helpful discussions with Ing. Patrick Markus from Veeco Instruments BV (Breda, The Netherlands). This work has been financially supported by the MESA$^+$ Institute for Nanotechnology of the University of Twente, the Dutch Polymer Institute (grant #DPI – 510, grant to GJV), and the Council for Chemical Sciences of the Netherlands Organization for Scientific Research (CW-NWO) in the framework of the *vernieuwingsimpuls* program (grant awarded to HS) and in the framework of the NWO middelgroot investment grant (grant 700.54.102).

Appendix A. Supplementary data

Supplementary data associated with this article can be found, in the online version, at doi:10.1016/j.eurpolymj.2007.07.035.

References

[1] Kroto HW, Heath JR, Obrien SC, Curl RF, Smalley RE. Nature 1985;318:162.
[2] Iijima S. Nature 1991;354:56.
[3] Saito R, Dresselhaus G, Dresselhaus MS. Physical properties of carbon nanotubes. London: Imperial College London; 1998.
[4] Baughman RH, Zakhidov AA, de Heer WA. Science 2002;297:787.

[5] Coleman JN, Khan U, Gun'ko YK. Adv Mater 2006;18:689.
[6] Aleshin AN. Adv Mater 2006;18:17.
[7] Besteman K, Lee JO, Wiertz FGM, Heering HA, Dekker C. Nano Lett 2003;3:727.
[8] Chen JY, Kutana A, Collier CP, Giapis KP. Science 2005;310:1480.
[9] Andrews R, Jacques D, Rao AM, Rantell T, Derbyshire F, Chen Y, et al. Appl Phys Lett 1999;75:1329.
[10] Gao JB, Itkis ME, Yu AP, Bekyarova E, Zhao B, Haddon RC. J Am Chem Soc 2005;127:3847.
[11] Jia ZJ, Wang ZY, Xu CL, Liang J, Wei BQ, Wu DH, et al. Mater Sci Eng A – Struct 1999;271:395.
[12] Moniruzzaman M, Winey KI. Macromolecules 2006;39:5194.
[13] Salvetat JP, Bhattacharyya S, Pipes RB. J Nanosci Nanotechnol 2006;6:1857.
[14] Tasis D, Tagmatarchis N, Bianco A, Prato M. Chem Rev 2006;106:1105.
[15] Gass MH, Koziol KKK, Windle AH, Midgley PA. Nano Lett 2006;6:376.
[16] Anderson N, Anger P, Hartschuh A, Novotny L. Nano Lett 2006;6:744.
[17] Ding W, Eitan A, Fisher FT, Chen X, Dikin DA, Andrews R, et al. Nano Lett 2003;3:1593.
[18] Shekhawat GS, Dravid VP. Science 2005;310:89.
[19] Taubner T, Keilmann F, Hillenbrand R. Opt Express 2005;13:8893.
[20] Hobbs JK, Register RA. Macromolecules 2006;39:703.
[21] Lammertink RGH, Hempenius MA, Manners I, Vancso GJ. Macromolecules 1998;31:795.
[22] Li L, Chan CM, Li JX, Ng KM, Yeung KL, Weng LT. Macromolecules 1999;32:8240.
[23] Magonov SN, Reneker DH. Annu Rev Mater Sci 1997;27:175.
[24] Pearce R, Vancso GJ. Macromolecules 1997;30:5843.
[25] Schonherr H, Wiyatno W, Pople J, Frank CW, Fuller GG, Gast AP, et al. Macromolecules 2002;35:2654.
[26] Postma HWC, Sellmeijer A, Dekker C. Adv Mater 2000;12:1299.
[27] Garcia R, Perez R. Surf Sci Rep 2002;47:197.
[28] James PJ, Antognozzi M, Tamayo J, McMaster TJ, Newton JM, Miles MJ. Langmuir 2001;17:349.
[29] Tamayo J, Garcia R. Appl Phys Lett 1997;71:2394.
[30] (a) For AFM work on CNT filled polymers, see also Cuberes MT, Assender HE, Briggs GAD, Kolosov OV. J Phys D Appl Phys 2000;33:2347;
(b) Satapathy BK, Weidisch R, Potschke P, Janke A. Macromol Rapid Commun 2005;26:1246;
(c) Loos J, Alexeev A, Grossiord N, Koning CE, Regev O. Ultramicroscopy 2005;104:160.
[31] DI/Veeco. Application note 42. Tunneling AFM and conductive AFM with NanoScope(R) AFM; 2000.
[32] Gautier B, Fares B, Prudon G, Dupuy JC. Appl Surf Sci 2004;231-2:136.
[33] Kelley TW, Granstrom EL, Frisbie CD. Adv Mater 1999;11:261.
[34] McEvoy TM, Long JW, Smith TJ, Stevenson KJ. Langmuir 2006;22:4462.
[35] Ravier J, Houze F, Carmona F, Schneegans O, Saadaoui H. Carbon 2001;39:314.
[36] Liu TX, Phang IY, Shen L, Chow SY, Zhang WD. Macromolecules 2004;37:7214.
[37] Zhang WD, Shen L, Phang IY, Liu TX. Macromolecules 2004;37:256.
[38] Phang IY, Ma JH, Shen L, Liu TX, Zhang WD. Polym Int 2006;55:71.
[39] Tivanski AV, Bemis JE, Akhremitchev BB, Liu HY, Walker GC. Langmuir 2003;19:1929.
[40] Gomez-Navarro C, Gil A, Alvarez M, De Pablo PJ, Moreno-Herrero F, Horcas I, et al. Nanotechnology 2002;13:314.
[41] Fasolka MJ, Mayes AM, Magonov SN. Ultramicroscopy 2001;90:21.
[42] Carmona F, Ravier J. Carbon 2002;40:151.
[43] Hu L, Hecht DS, Gruner G. Nano Lett 2004;4:2513.
[44] Kirkpatrick S. Rev Mod Phys 1973;45:574.
[45] Fuchs H, Eng LM, Sander R, Petermann J, Jandt KD, Hoffmann T. Polym Bull 1991;26:95.